Original Article

# Angiopoietin-like 4 directs uptake of dietary fat away from adipose during fasting

CrossMark

Emily M. Cushing [a], Xun Chi [a], Kelli L. Sylvers [a], Shwetha K. Shetty [a], Matthew J. Potthoff [b], Brandon S.J. Davies [a],[*]

## ABSTRACT

**Objective:** Angiopoietin-like 4 (ANGPTL4) is a fasting-induced inhibitor of lipoprotein lipase (LPL) and a regulator of plasma triglyceride metabolism. Here, we examined the kinetics of *Angptl4* induction and tested the hypothesis that ANGPTL4 functions physiologically to reduce triglyceride delivery to adipose tissue during nutrient deprivation.

**Methods:** Gene expression, LPL activity, and triglyceride uptake were examined in fasted and fed wild-type and *Angptl4*$^{-/-}$ mice.

**Results:** *Angptl4* was strongly induced early in fasting, and this induction was suppressed in mice with access to food during the light cycle. Fasted *Angptl4*$^{-/-}$ mice manifested increased LPL activity and triglyceride uptake in adipose tissue compared to wild-type mice.

**Conclusions:** *Angptl4* is induced early in fasting to divert uptake of fatty acids and triglycerides away from adipose tissues.

© 2017 The Authors. Published by Elsevier GmbH. This is an open access article under the CC BY-NC-ND license (http://creativecommons.org/licenses/by-nc-nd/4.0/).

**Keywords** Plasma triglycerides; Lipoprotein metabolism; Lipolysis; Lipase inhibition

## 1. INTRODUCTION

Misregulation of plasma triglyceride metabolism and fatty acid delivery has been implicated in several metabolic diseases, including metabolic syndrome, diabetes mellitus, and atherosclerosis [1,2]. The enzyme lipoprotein lipase (LPL) is positioned at the nexus of plasma triglyceride delivery, hydrolyzing plasma lipoprotein triglycerides and releasing fatty acids for uptake into heart, skeletal muscle, and adipose tissue. LPL-mediated hydrolysis normally occurs on the luminal surface of capillary endothelial cells where LPL is anchored by GPIHBP1, an endothelial cell GPI-anchored protein responsible for transporting LPL across endothelial cells [3,4].

Angiopoietin-like 4 (ANGPTL4), also known as fasting-inducible adipose factor (FIAF), is a fasting induced inhibitor of LPL and a regulator of triglyceride metabolism [5–7]. ANGPTL4 is most highly expressed in adipose tissue and liver, but it is also expressed at lower levels in muscle, heart, kidney, and intestine [5,8], and circulates in plasma [5]. Plasma triglycerides are elevated in mice overexpressing ANGPTL4, whereas *Angptl4*$^{-/-}$ mice display reduced plasma triglyceride levels [7]. ANGPTL4 inactivates LPL by accelerating the dissociation of active LPL dimers to inactive monomers [9]. ANGPTL4 expression increases markedly upon fasting leading to the hypothesis that ANGPTL4 is involved in regulating fatty acid delivery in the fasted state [5].

In humans, inactivating mutations in ANGPTL4 are associated with lower plasma triglycerides [10–12] and lower incidence of coronary artery disease [11–13]. Thus, it has been proposed that targeting ANGPTL4 activity may be a useful way to therapeutically increase LPL-driven triglyceride clearance, lower plasma triglycerides, and lower the risk of coronary disease [11,12,14,15]. However, as LPL-driven ectopic lipid deposition can potentially lead to detrimental effects, including skeletal muscle insulin resistance [16], cardiac lipotoxicity [17], and severe inflammatory responses [18], understanding where and when ANGPTL4 normally acts is essential.

In this study, we investigate the physiological mechanisms by which ANGPTL4 regulates plasma triglycerides. We analyze the tissue-specific kinetics of fasting-induced *Angptl4* gene expression, and examine the effects of ANGPTL4 deficiency on tissue-specific lipase activity and triglyceride delivery.

## 2. MATERIALS AND METHODS

### 2.1. Mice

All animal procedures were approved by the Institutional Animal Care and Use Committee at the University of Iowa and were carried out in accordance with the National Institutes of Health Guide for the Care and Use of Laboratory Animals. Mice were group housed in a controlled environment with a 12/12 light/dark cycle, with food and water provided *ad libitum* during non-fasting conditions. During fasting conditions, water was provided *ad libitum*.

[a]Department of Biochemistry, Fraternal Order of Eagles Diabetes Research Center, Obesity Research and Education Initiative, University of Iowa Carver College of Medicine, 169 Newton Rd, Iowa City, IA 52242, United States [b]Department of Pharmacology and Fraternal Order of Eagles Diabetes Research Center, University of Iowa Carver College of Medicine, 169 Newton Rd, Iowa City, IA 52242, United States

*Corresponding author. Department of Biochemistry, 169 Newton Rd, PBDB 3326, Iowa City, IA 52242, United States. E-mail: Brandon-davies@uiowa.edu (B.S.J. Davies).

*Abbreviations:* ANGPTL4, angiopoietin-like 4; LPL, lipoprotein lipase; GPIHBP1, glycosylphosphatidylinositol-anchored high-density lipoprotein binding protein 1; sWAT, subcutaneous white adipose tissue; gWAT, gonadal white adipose tissue; mWAT, mesenchymal white adipose tissue; BAT, brown adipose tissue

C57BL/6J mice were obtained from Jackson Laboratories. $Gpihbp1^{-/-}$ mice (B6;129S5-$Gpihbp1^{tm1Lex}$/Mmucd) [19,20], and $Angptl4^{-/-}$ mice (B6;129S5-$Angptl4^{Gt(OST352973)Lex}$/Mmucd) [19,21] were generated by breeding from strains obtained from the Mutant Mouse Resource and Research Center (mmrrc.org). Age-matched wild-type littermates were used as controls for $Angptl4^{-/-}$ mice.

## 2.2. Plasma triglyceride assays
$Angptl4^{-/-}$ mice and wild-type littermates were fasted for 4 h (fasted group) or fasted for 6 h and then fed normal chow for 2 h (refed group). Blood was collected via tail-nick into EDTA-coated collection tubes. After centrifugation at $1500 \times g$ for 15 min at 4 °C to pellet the cells, plasma from each mouse was combined with Infinity™ Triglyceride Reagent (Thermo Scientific TR22421) according to the manufacturer's instructions. Samples were incubated at 37 °C for 10 min and absorbance was measured at 500 nm. Triglyceride concentrations were determined by comparison to a standard curve prepared from a triolein standard (Nu-Chek Prep, Lot T-235-N13-Y).

## 2.3. RNA isolation and qPCR analysis
Mouse tissue samples were frozen in liquid nitrogen and pulverized using a Bessman tissue pulverizer. Crushed tissue was resuspended in Trizol (Ambion, 15596-018) and processed according to the manufacturer's instructions. After assessing mRNA concentration and quality using a Nanodrop spectrophotometer (ThermoScientific), cDNA was prepared using the High Capacity cDNA Reverse Transcription kit (Applied Biosystems, Part No. 4368813). qPCR was performed (Invitrogen, SYBR GreenER qPCR Supermix, 11762100) according to the manufacturer's specifications using an Applied Biosystems 7900HT Fast Real-Time PCR System (Iowa Institute of Human Genetics). Relative expression was calculated with the $\Delta\Delta$ct method [22] using $CycloA$ as the reference gene.

## 2.4. Lipase activity assay
Frozen tissue samples were crushed and resuspended in LPL assay buffer (25 mM $NH_4Cl$, 5 mM EDTA, 0.01% SDS, 45 U/mL heparin, 0.05% 3-(N,N-Dimethylmyristylammonio) propanesulfonate zwittergent detergent (Acros Organics, 427740050)) containing Mammalian ProteaseArrest (GBiosciences, cat no. 786-331). The tissue suspension was mixed by vortexing and incubated on ice for 30 min, with intermittent disruption with surgical scissors. The resulting lysate was centrifuged at $15,000 \times g$ for 15 min at 4 °C to pellet cellular debris. Lipase activity assays were performed on the supernatants as previously described [23]; supernatants were combined with a working buffer composed of 0.6 M NaCl, 80 mM Tris–HCl pH 8, 6% fatty-acid free BSA and an EnzChek lipase fluorescent substrate (Molecular Probes, E33955). Fluorescence was measured over 30 min at 37 °C on a SpectraMax i3 plate reader (Molecular Devices). Relative lipase activity was calculated by subtracting background (calculated by reading fluorescence of a sample with no LPL) and then calculating the slope of the curve between the 5 and 13 min reads. The data were graphed as the average of slopes for each group.

## 2.5. Preparation of ^{3}H-Labeled intralipid
[3]H-Intralipid was prepared by mixing [9,10-3H(N)]-Triolein (Perkin Elmer, NET431001MC) with 5% Intralipid (prepared fresh from Intralipid® 20% (NDC 0338-0519-03)) in a ratio of 1 μCi triolein to 10 μL of Intralipid. The mixture was sonicated briefly on low power 3 × 20 s, with 1 min on ice between each round of sonication. The mixture was

centrifuged briefly and diluted 10-fold in saline to prepare a 0.5% stock.

## 2.6. Preparation of ^{3}H-Labeled chylomicrons
$Gpihbp1^{-/-}$ mice were fasted 4 h and then gavaged with 100 μCi of [9,10-3H(N)]-Triolein (Perkin Elmer, NET431001MC) suspended in olive oil. After 4 h, mice were anesthetized, and blood was collected by cardiac puncture. Blood was diluted 1:10 with 0.5 M EDTA (pH 8.0) and centrifuged $1500 \times g$ for 15 min at 4 °C to pellet blood cells. The plasma was then transferred to ultracentrifuge tubes and mixed 1:1 with PBS. After centrifugation at $424,000 \times g$ for 2 h at 10 °C, the chylomicrons form an upper layer. The chylomicron layer was resuspended in fresh PBS and the centrifugation was repeated. Following the second centrifugation, the chylomicron layer was resuspended in PBS to the original plasma volume. Protein content was assayed using the BioRAD DC Protein Assay (BioRAD, 5000116). Radioactivity was determined in BioSafe II scintillation fluid (RPI, 111195) on a Beckman-Coulter Liquid Scintillation Counter (BCLSC6500).

## 2.7. Triglyceride clearance assay
Wild-type and $Angptl4^{-/-}$ mice were fasted 4 h (fasted group) or were fasted for 6 h and then returned to chow for 2 h (refed group). Mice were anesthetized with isoflurane and injected retro-orbitally with 200 μL 0.5% ^{3}H-Intralipid (see Section 2.5) or 100 μL of ^{3}H-chylomicron suspension (see Section 2.6). Proparacaine hydrochloride ophthalmic solution, USP 0.5% (AKORN, 17478-263-12) was used to minimize discomfort both during and after injection. Blood samples were taken via tail-nick at 1, 5, 10, and 15 min after injection. Blood samples were assayed in BioSafe II scintillation fluid on a Beckman-Coulter Scintillation Counter. After the last blood draw, the mice were anesthetized with isoflurane, and tissues were harvested and weighed. A portion of each tissue was then weighed and placed in 2:1 chloroform:methanol overnight at 4 °C. 1 mL of 2 M $CaCl_2$ was then added to each sample to separate organic and aqueous layers. The samples were centrifuged for 10 min at 1500 rpm, and the upper aqueous layer was mixed with BioSafe II scintillation fluid and assayed on a Beckman-Coulter Scintillation Counter. The lower organic layer was evaporated overnight to remove chloroform, and the remaining sample was resuspended in scintillation fluid and assayed in BioSafe II scintillation fluid on a Beckman-Coulter Liquid Scintillation Counter. Aqueous and organic fractions were combined to obtain the total uptake CPM. CPM were measured for an aliquot representing 10% (by volume) of the chylomicrons injected into each mouse. This value was used to normalize the radiolabel data across mice.

## 2.8. Triglyceride uptake after gavage with ^{3}H-Triolein
Wild-type and $Angptl4^{-/-}$ mice were fasted 4 h, beginning at the onset of the light cycle. After 4 h, the mice were gavaged with 2 μCi of [9,10-3H(N)]-Triolein (Perkin Elmer, NET431001MC) in 100 μL olive oil. After 4 h, the mice were anesthetized with isoflurane, and tissues were harvested and weighed. Tissues were then analyzed for radiolabel as described in Section 2.7.

## 2.9. Statistics and outlier identification
Statistics and outlier identification were performed using Graphpad Prism. Statistical significance was tested using Student's T-test unless otherwise indicated. Outliers were identified using Grubbs test and were excluded from graphs and from statistical analysis. The number

of mice analyzed for each experiment ranged from 4 to 10 and is specified in each figure legend.

## 3. RESULTS

### 3.1. *Angptl4* expression is induced early in fasting

Consistent with previous reports [5], we found that *Angptl4* expression in mice after a 24 h fast was upregulated in several tissues including heart, liver, and adipose tissue (Figure 1A). Because longer fasts induce a catabolic state in mice [24], we asked at what point during the

fast *Angptl4* was upregulated. We began fasting mice at the beginning of their light cycle and measured *Angptl4* expression after 0, 2, 4, 6, 8, 10, and 12 h. After 12 h of fasting, food was restored to the remaining mice and *Angptl4* expression was measured 2 or 4 h after this refeeding (Figure 1B). Surprisingly, *Angptl4* expression was already highly induced at the 2 h time point in all tissues (Figure 1C). In most tissues, expression gradually declined after the 2 h time point and returned to baseline or lower after refeeding.

To investigate the possibility that the increased *Angptl4* expression at 2 h was the result of circadian regulation at the onset of the light cycle,
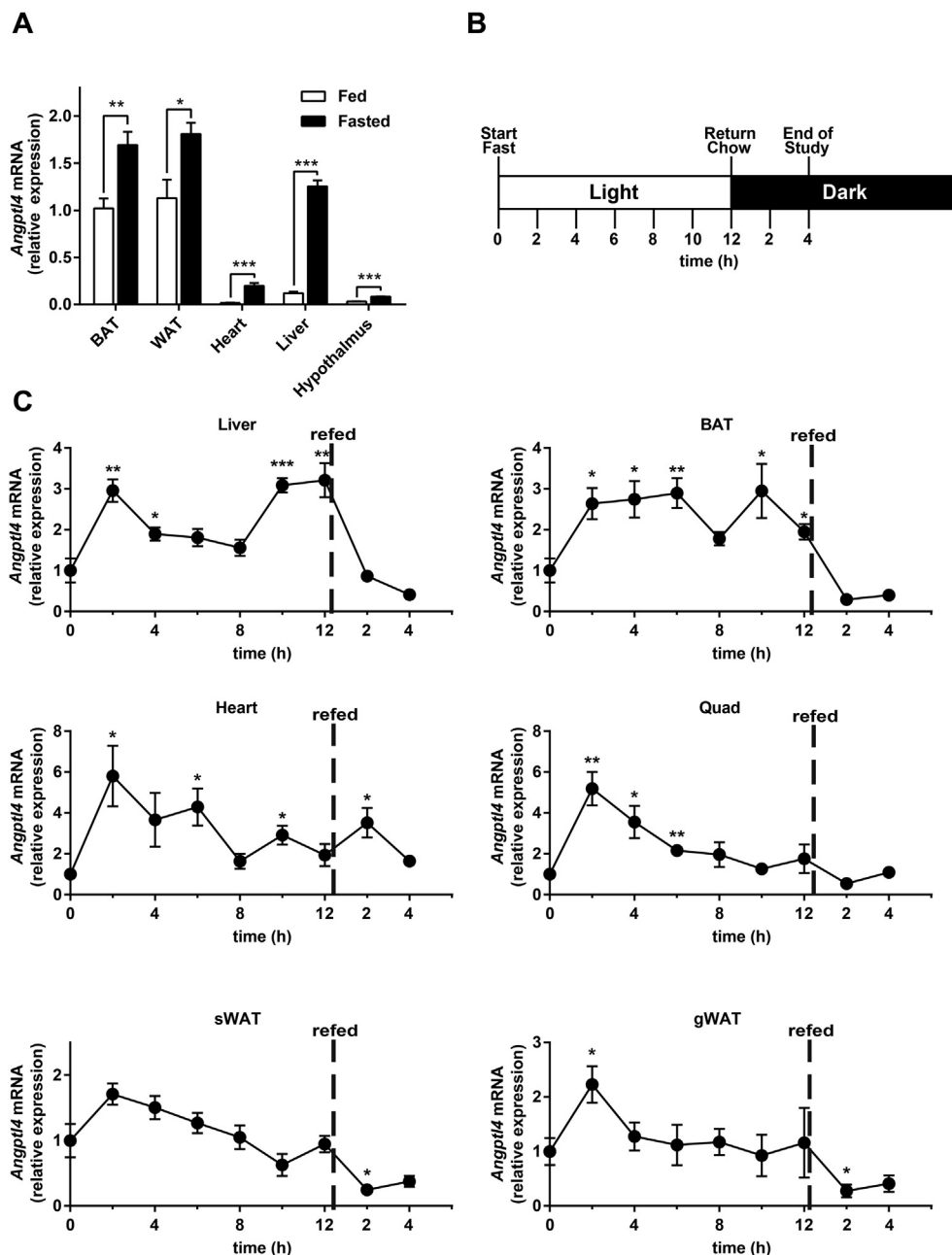


**Figure 1:** Induction of *Angptl4* expression by fasting. (**A**) Male C57/Bl6 mice (n = 5/group were fed *ad lib* or fasted for 24 h. *Angptl4* expression in BAT, WAT, heart, liver, and hypothalamus (mean ± SEM; *p < 0.05, **p < 0.01, ***p < 0.001). (**B**) Experimental design for fasting time course; male C57/Bl6 mice (n = 5/time point) were fasted at the onset of the light cycle and sacrificed after 0, 2, 4, 6, 8, 10, or 12 h of fasting, or after a 12 h fast, and 2 or 4 h of refeeding. (**C**) Expression of *Angptl4* in liver, brown adipose tissue (BAT), heart, quadriceps, subcutaneous white adipose tissue (sWAT), and gonadal WAT (gWAT) in mice subjected to the fasting time course depicted in (B). Points show expression relative to time 0 (mean ± SEM; *p < 0.05, **p < 0.01, ***p < 0.001 when compared to time 0).

rather than the result of actual fasting, we compared *Angptl4* expression at the same time points during the light cycle for mice that were fasted or allowed to feed *ad lib* (Figure 2A). For fasted mice, food was withdrawn at the beginning of the light cycle, and *Angptl4* expression was assessed for both fasted and fed mice after 2 and 12 h. Although mice typically eat less during the light cycle, the mice with access to food showed no significant upregulation of *Angptl4* expression at either 2 or 12 h (Figure 2B). However, consistent with our previous results, *Angptl4* expression was upregulated after 2 h in the fasted mice (Figure 2B). These data strongly suggest that fasting itself, not circadian cycles, drives increased *Angptl4* expression.

### 3.2. *Angptl4*$^{-/-}$ mice have reduced plasma triglycerides in the fasted state

To examine the physiological role of ANGPTL4 in triglyceride metabolism and fatty acid delivery, we used *Angptl4*$^{-/-}$ mice. As expected,
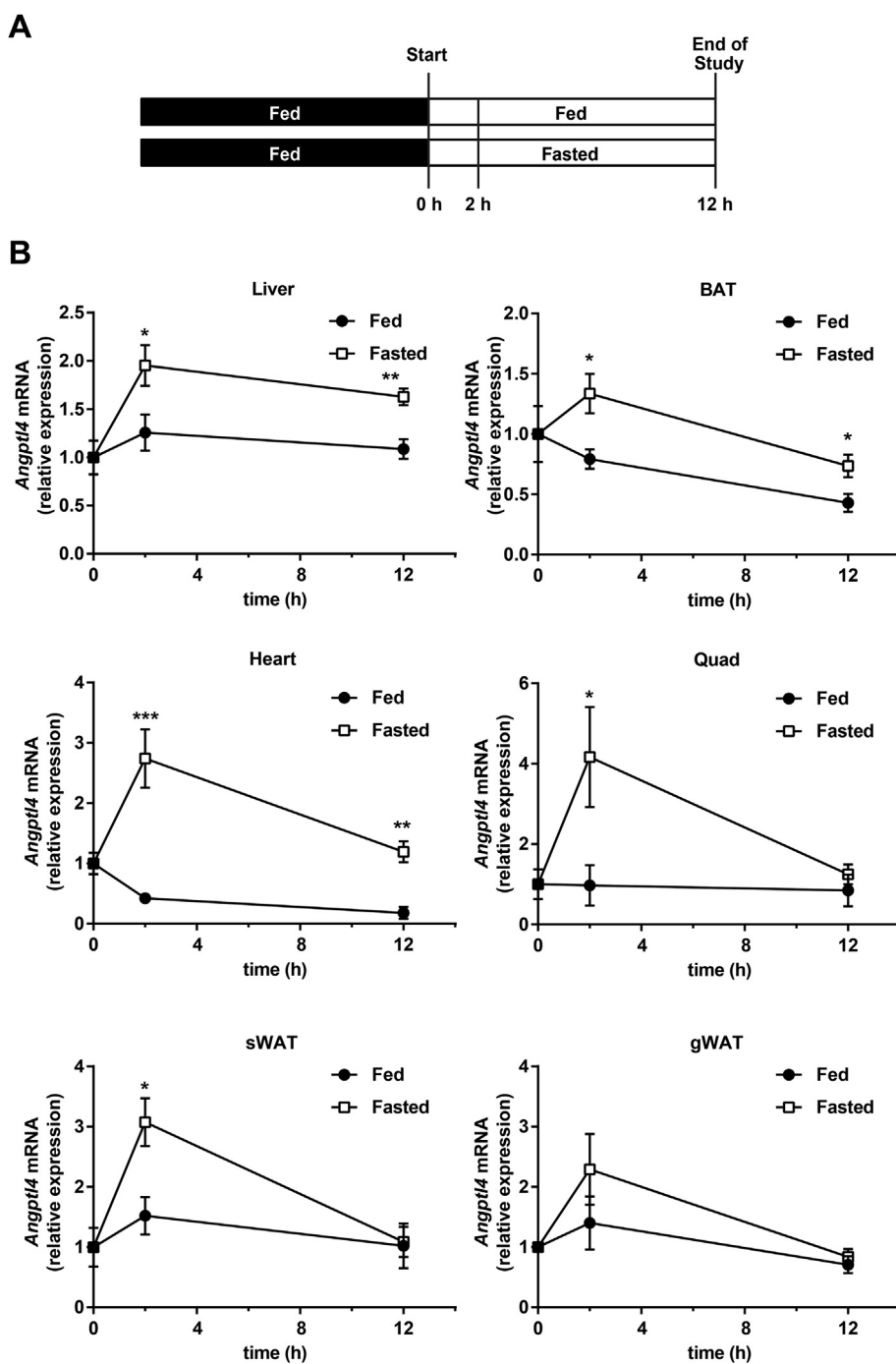


**Figure 2:** Expression of *Angptl4* is fasting induced, rather than circadian. (**A**) Diagram depicts mouse light cycle and experimental design for (B); tissues from wild-type mice (n = 6/group) were harvested at 0, 2, or 12 h, either after fasting or *ad lib* access to chow. (**B**) *Angptl4* expression in liver, brown adipose tissue (BAT), heart, quadriceps (quad), subcutaneous white adipose tissue (sWAT), and gonadal white adipose tissue (gWAT). Points show expression relative to time 0 (mean ± SEM; *p < 0.05, **p < 0.01, ***p < 0.001 when comparing fasted to fed mice at the same time point).

*Angptl4*⁻/⁻ mice did not express *Angptl4*, whereas in wildtype littermates, *Angptl4* expression was easily detectable, and was higher after a 4 h fast than after refeeding (Figure 3A). *Angptl4*⁻/⁻ mice had lower serum triglyceride levels than wild-type litter mates after a 4 h fast (Figure 3B), consistent with the established idea that ANGPTL4-deficiency results in increased LPL activity and thus, increased triglyceride clearance in the fasted state. Notably, no significant difference was observed in triglyceride levels between wild-type and *Angptl4*⁻/⁻ mice in refed mice (6 h fast, 2 h refeed), a time when *Angptl4* expression is reduced (Figure 3B).

Gene expression of the LPL transporter GPIHBP1 also increases after an overnight fast [25]. It had previously been reported that ANGPTL4-deficiency disrupts this increase [26], we did not observe this to be the case. After a 16 h fast, *Gpihbp1* expression responded similarly in both *Angptl4*⁻/⁻ and wild-type mice (Supplemental Figure 1A and B).

### 3.3. Triglyceride clearance is increased in the adipose depots of *Angptl4*⁻/⁻ mice

Given that ANGPTL4 inhibits LPL activity [6,7,9], the reduced plasma triglycerides in *Angptl4*⁻/⁻ mice are likely the result of increased LPL-

mediated triglyceride hydrolysis and fatty acid uptake. To determine the fate of triglyceride-derived fatty acids in *Angptl4*⁻/⁻ mice, and thus the likely location of ANGPTL4 action, we performed triglyceride clearance assays in wild-type and *Angptl4*⁻/⁻ mice using Intralipid spiked with radiolabeled triolein. We reasoned that the tissues in which there is the greatest ANGPTL4 inhibitory activity would manifest the greatest increase in radiolabel uptake in *Angptl4*⁻/⁻ mice. Thus, if circulating endocrine ANGPTL4 is primarily responsible for LPL inhibition, tissues with the greatest LPL activity (heart, adipose tissue, skeletal muscle) would have increased radiolabeled uptake in *Angptl4*⁻/⁻ versus wild-type mice. Whereas, if ANGPTL4 acts locally to inhibit LPL, we would expect tissues with the greatest expression of ANGPTL4, particularly adipose tissue, to have the greatest increase in radiolabel uptake in *Angptl4*⁻/⁻ mice. Our data strongly supported the latter possibility, as we observed increased radiolabel uptake exclusively in the adipose tissues of *Angptl4*⁻/⁻ mice (Figure 4). Uptake into heart was decreased and was unchanged in liver, kidney, and muscle (Figure 4).

### 3.4. Chylomicron clearance is increased in the white adipose tissue of *Angptl4*⁻/⁻ mice primarily in the fasted state

Because Intralipid emulsions lack many properties of triglyceride-rich lipoproteins, including the presence of apolipoproteins, we performed triglyceride clearance assays using radiolabeled chylomicrons. Radiolabeled chylomicrons were isolated from the plasma of *Gpihbp1*⁻/⁻ mice fed ³H-triolein (see Section 2.6). Fasted (4 h) and refed (6 h fast, 2 h refeed) *Angptl4*⁻/⁻ and wild-type littermate mice were injected intravenously with radiolabeled chylomicrons. Triglyceride clearance from the circulation was measured by taking blood samples 1, 5, 10, and 15 min after injection. After 15 min, tissues were harvested and the amount of radiolabel was measured to determine uptake into individual tissue. Experiments were performed in both male and female mice.

In female mice, radiolabel clearance from the plasma was faster in *Angptl4*⁻/⁻ mice than in wild-type mice, but only in the fasted state (Figure 5A). In wild-type female mice, triglyceride uptake into white adipose tissue was significantly elevated in the refed state, whereas uptake into the heart decreased (Figure 5B–I). Consistent with the Intralipid uptake data (Figure 3B), radiolabel uptake into adipose tissue in the fasted state was significantly higher in female *Angptl4*⁻/⁻ mice than in wild-type mice (Figure 5D–F). Unlike wild-type mice, radiolabel uptake into the white adipose tissue of *Angptl4*⁻/⁻ mice did not significantly increase in the refed state. Interestingly, radiolabel uptake into adipose tissue after refeeding was not significantly different between wild-type and *Angptl4*⁻/⁻ mice, supporting the idea that ANGPTL4 regulates triglyceride metabolism primarily in the fasted state (Figure 5D–F). In female mice, radiolabel uptake into liver, kidney, brown adipose tissue, and skeletal muscle, did not differ significantly between wild-type and *Angptl4*⁻/⁻ mice (Figure 5A, B, H, I).

In male mice, no significant differences in the rate of plasma triglyceride clearance were observed (Figure 6A). As in female mice, fasted *Angptl4*⁻/⁻ mice had reduced radiolabel uptake into heart and increased uptake into gonadal white adipose tissue (gWAT) and subcutaneous white adipose tissue (sWAT) when compared to fasted wild-type mice (Figure 6D, E, G). Interestingly, in the gWAT and sWAT of male mice, the differences in uptake between *Angptl4*⁻/⁻ and wild-type mice persisted in the refed state (Figure 6D, E). As in female mice, there were no differences between *Angptl4*⁻/⁻ and wild-type mice in radiolabel uptake into liver, kidney, skeletal muscle, or brown adipose tissue (Figure 6).

**A**



**B**
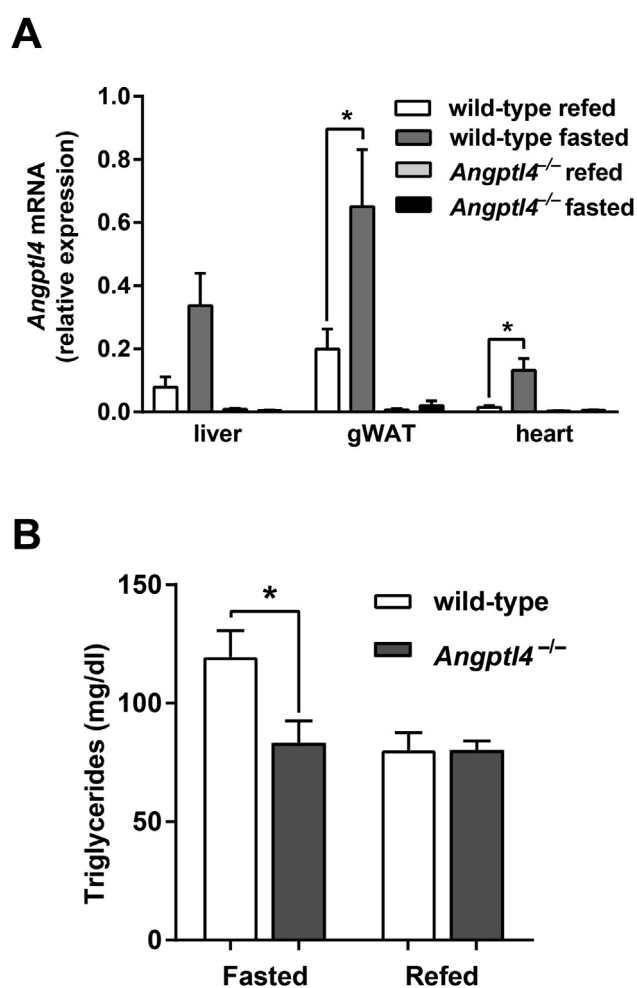


**Figure 3:** Fasted plasma triglycerides are lower in *Angptl4*⁻/⁻ mice than in wild-type mice. ANGPTL4 expression in liver, gonadal white adipose tissue (gWAT) and liver (**A**) and plasma triglyceride levels (**B**) of female *Angptl4*⁻/⁻ and wild-type littermate mice that were fasted 4 h (fasted group) or fasted 6 h and allowed to feed *ad lib* for 2 h (refed) (n = 5—8/group). Bar graphs show mean ± SEM (*p < 0.05).
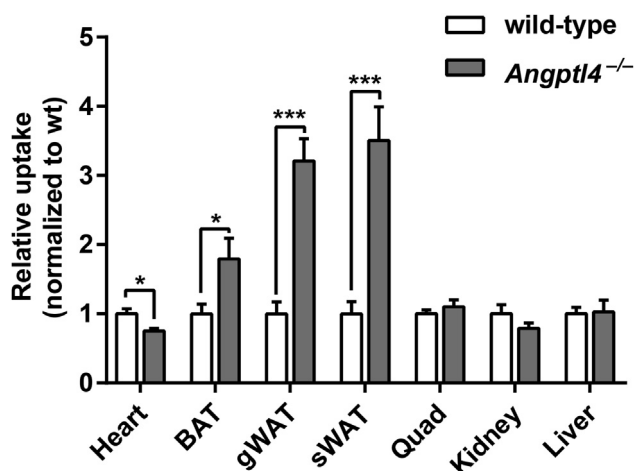
**Figure 4:** *Angptl4⁻ᐟ⁻* mice show increased uptake of triglyceride to adipose tissue compared to wild-type mice. Radiolabel uptake into tissues after 15 min in male wild-type and *Angptl4⁻ᐟ⁻* mice that had been fasted 4 h and injected intravenously with Intralipid spiked with ³H-triolien (n = 6/group). Bars show relative radiolabel uptake per mg tissue normalized to wild-type (mean ± SEM; **p < 0.01, ***p < 0.001).

We also tested triglyceride clearance after an oral gavage of ³H-triolein. Male mice were fasted 4 h and then administered ³H-triolein in olive oil by oral gavage. Tissues were harvested 4 h after gavage, and the amount of radiolabel was measured to determine uptake into individual tissue. Consistent with our previous observations, we found reduced radiolabel uptake in heart and increased uptake in adipose tissue (Figure 7). Together these data indicate that the lower plasma triglyceride levels in *Angptl4⁻ᐟ⁻* mice are a result of increased uptake into adipose tissue.

### 3.5. Lipase activity is increased in the adipose depots of *Angptl4⁻ᐟ⁻* mice

To verify that the increased uptake of triglyceride-derived fatty acids into adipose tissue in *Angptl4⁻ᐟ⁻* mice was the result of decreased inhibition of LPL, we also measured heparin-releasable lipase activity in the tissue of fasted wild-type and *Angptl4⁻ᐟ⁻* mice. Lipase activity was greater in the white adipose tissue of *Angptl4⁻ᐟ⁻* mice, consistent with the idea that the absence of ANGPTL4 in adipose tissue leads to increased LPL activity and great triglyceride uptake in these tissues (Figure 8). Interestingly, lipase activity was unchanged in the hearts of *Angptl4⁻ᐟ⁻* mice, suggesting that the reduction of fasting triglyceride
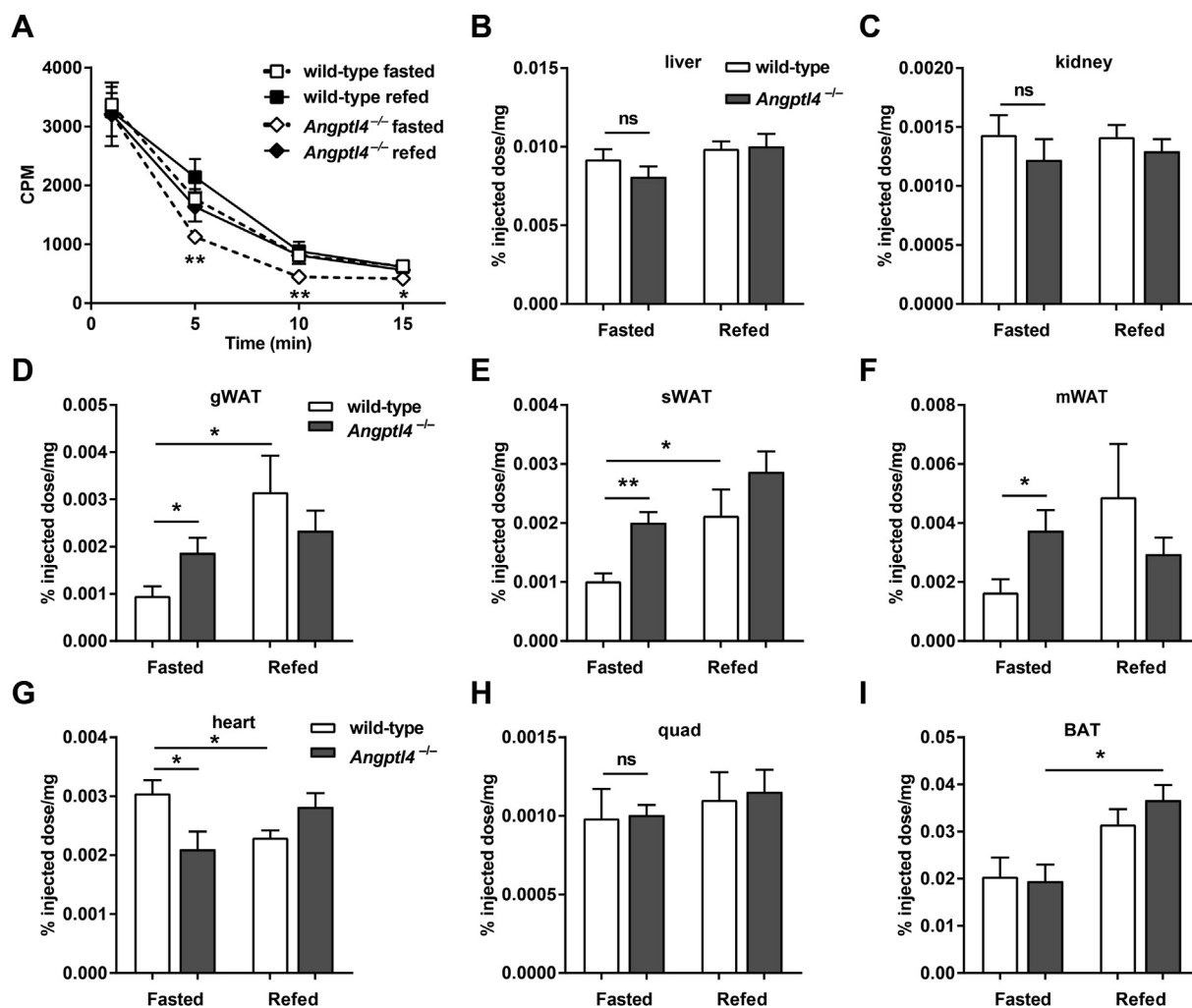


**Figure 5:** Chylomicron clearance and uptake in female wild-type and *Angptl4⁻ᐟ⁻* mice. Fasted (4 h) and refed (6 h fast 2 h fed) female mice were injected intravenously with ³H-triglyceride containing chylomicrons (n = 6/group). (**A**) Clearance of radiolabel from the plasma 1, 5, 10, and 15 min after injection. Points represent counts per minute (CPM) in 10 μl plasma at the indicated time points (mean ± SEM; *p < 0.05, **p < 0.01). (**B–I**) Uptake of radiolabel after 15 min (% injected dose/mg tissue) into the tissues of wild-type and *Angptl4⁻ᐟ⁻* mice (mean ± SEM; *p < 0.05, **p < 0.01).
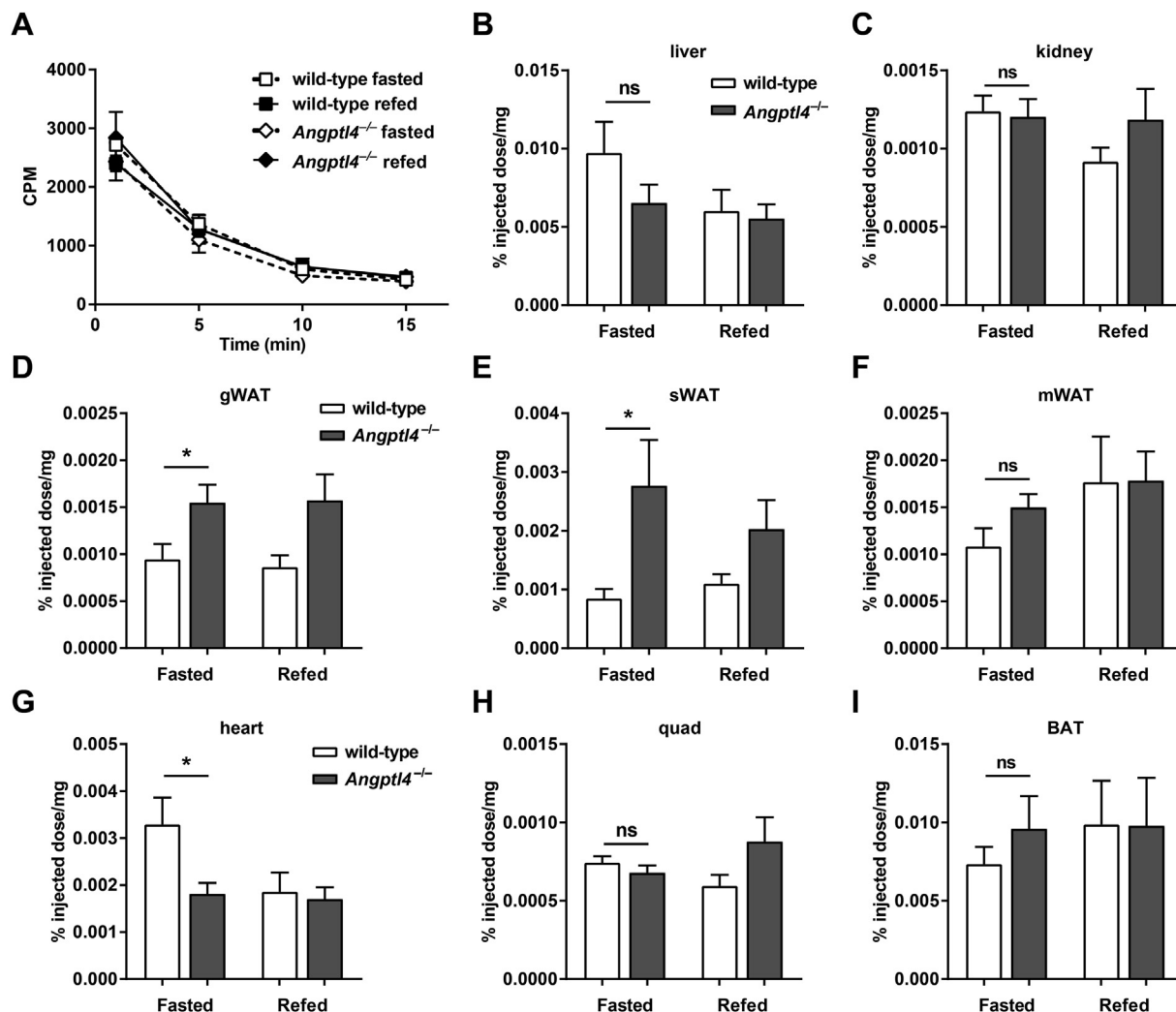
**Figure 6:** Chylomicron clearance and uptake in male wild-type and *Angptl4*$^{-/-}$ mice. Fasted (4 h) and refed (6 h fast 2 h refed) male mice were injected intravenously with $^3$H-triglyceride containing chylomicrons (n = 6/group). (**A**) Clearance of radiolabel from the plasma 1, 5, 10, and 15 min after injection. Points represent counts per minute (CPM) in 10 μl plasma at the indicated time points (mean ± SEM). (**B–I**) Uptake of radiolabel after 15 min (% injected dose/mg tissue) into the tissues of wild-type and *Angptl4*$^{-/-}$ mice (mean ± SEM; *p < 0.05).

uptake in these mice is primarily a result of increased uptake in adipose tissue rather than a change in cardiac lipase activity.

## 4. DISCUSSION

Although the induction of *Angptl4* expression by fasting has been demonstrated by several previous studies [5,7,26], the rapidity of *Angptl4* induction has not been fully appreciated. Initial reports looked at *Angptl4* expression after 24 h [5,27] or overnight [7] fasts. Here we demonstrated that *Angptl4* expression is induced after only 2 h of fasting, long before the mice enter a catabolic state. This contrasts with other fasting-induced factors, such as FGF21 or PPARα, which are induced after fasts of 8 h or longer [28—30]. Somewhat surprisingly, *Angptl4* was not induced during the light cycle if mice had access to food, despite the fact that mice generally eat far less during the light cycle. These data suggest that while ANGPTL4 is induced rapidly upon true fasting, even a low level of feeding is sufficient to abolish this induction. A limitation of our study is that we primarily measure gene expression. We attempted to also measure protein levels but of the

many commercial antibodies we tested none were specific for ANGPTL4 in mouse tissues (as judged by using *Angptl4*$^{-/-}$ mice as a negative control).

In this study, we used chylomicrons collected from *Gpihbp1*$^{-/-}$ mice to assess chylomicron clearance and fatty acid uptake. Doing so allowed us to use physiologically accurate chylomicrons rather than triglyceride emulsions [31—33] or "reconstituted" lipoproteins [34,35]. Our data from this and other assays suggest that ANGPTL4 mediates its effects on plasma triglyceride levels and fatty acid delivery primarily in the fasted state. Female *Angptl4*$^{-/-}$ mice had lower plasma triglycerides than wild-type, but only in the fasted state. Likewise, fatty acid delivery to tissues in female *Angptl4*$^{-/-}$ mice was only significantly different from that in wild-type mice in the fasted state. This was also the case in male mice; however, for these mice, a trend towards increased triglyceride uptake into adipose tissue persisted two hours after refeeding, indicating that there may be gender specific differences in the kinetics of the refeeding response. Additional studies are necessary to determine whether ANGPTL4 kinetics may also be altered in females during other metabolic states including pregnancy.
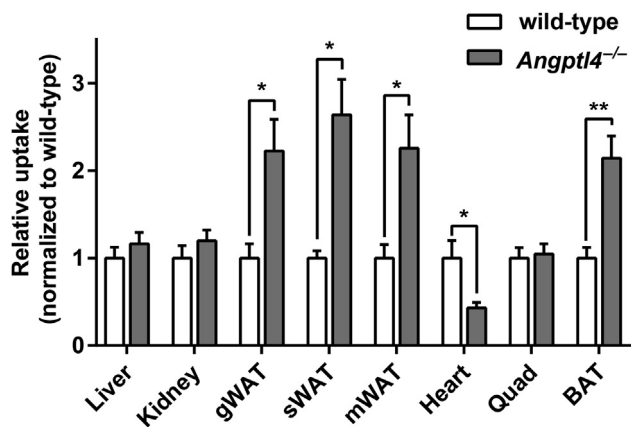
**Figure 7:** Triglyceride clearance after oral gavage in male wild-type and *Angptl4*$^{-/-}$ mice. Radiolabel uptake into tissues after 4 h in male wild-type and *Angptl4*$^{-/-}$ mice that had been fasted 4 h and orally gavaged with olive oil spiked with $^3$H-triolein (n = 4–6/group). Bars show relative radiolabel uptake per mg tissue normalized to wild-type (mean ± SEM; *p < 0.05, **p < 0.01).
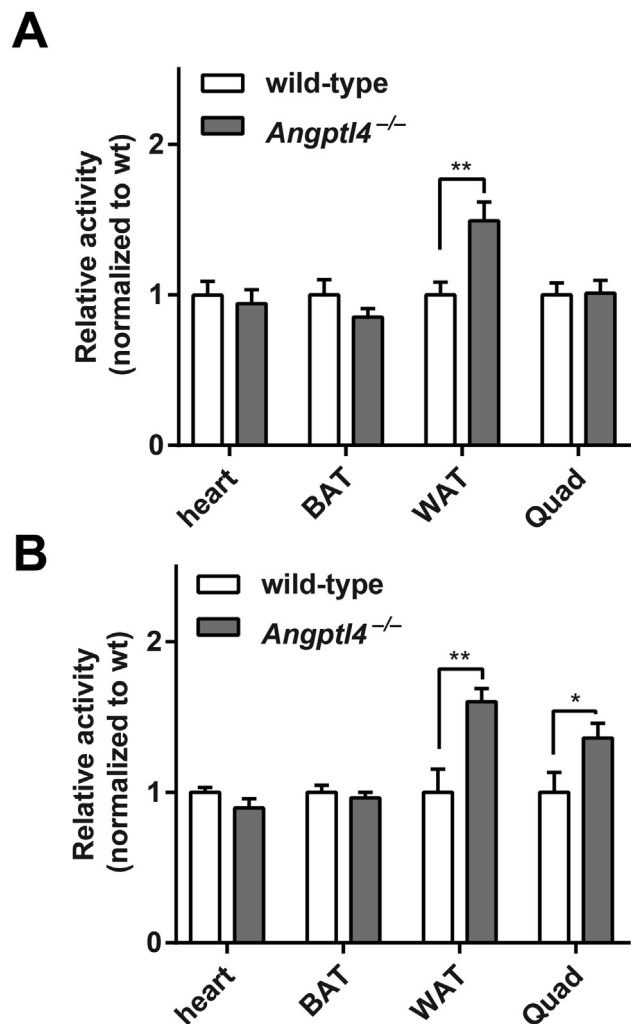


**Figure 8:** Lipase activity in male and female *Angptl4*$^{-/-}$ mice. Female (**A**) and male (**B**) wildtype and *Angptl4*$^{-/-}$ mice (6–10/group) were fasted for 4 h. Heart, brown adipose tissue (BAT), subcutaneous adipose tissue (WAT), and quadriceps (quad) were harvested and lipase activity was measured. Bars show relative lipase activity in each tissue normalized to wild-type (mean ± SEM; *p < 0.05, **p < 0.01).

Deficiency in ANGPTL4 increased lipase activity and triglyceride-derived fatty acid uptake primarily in adipose tissue, indicating that this is the primary location of ANGPTL4 action in regulating triglyceride metabolism. ANGPTL4 is expressed in adipose tissue at much high levels than in other tissues [5]. It is also important to note that vascular LPL is partially protected from ANGPTL4 by its endothelial cell transporter GPIHBP1 [23,36], but that adipose-expressed ANGPTL4 could act on LPL before LPL binds GPIHBP1. Indeed, recent studies have shown that adipocyte-expressed ANGPTL4 can inhibit LPL even before LPL is secreted [37]. Together these observations strongly suggest that the ANGPTL4 acting in adipose tissue is locally expressed. Although generation of an ANGPTL4 conditional allele and specific knockout of ANGPTL4 in adipose tissue will likely be needed to completely settle the issue, nonetheless, we predict that adipocyte-expressed ANGPTL4 is the major driver of the plasma triglyceride phenotypes observed in ANGPTL4 knockout mice as well as the shifts in fatty acid delivery observed during fasting.

Our studies support a model in which ANGPTL4 primarily acts locally in adipose tissue to inhibit LPL, and thus triglyceride uptake, during fasting. This inhibition would redirect triglyceride-derived fatty acids to tissues such as heart and muscle. Upon refeeding, ANGPTL4 inhibition of LPL ceases in adipose tissue, and at the same time inhibition of LPL by ANGPTL3 and ANGPTL8 increases in heart and skeletal muscle [38,39]. Thus, delivery of triglyceride-derived fatty acids to heart and skeletal muscle would slow and more fatty acids would be delivered to adipose tissue for storage.

Although *Angptl4* is highly expressed in adipose tissue, it is also expressed at lower levels in other tissues and cell types, including liver, skeletal muscle, heart, and macrophages [38]. If, as we propose, adipose ANGPTL4 is primarily responsible for plasma triglyceride and tissue fatty-acid uptake phenotypes in *Angptl4*$^{-/-}$ mice, what is the role of ANGPTL4 in other tissues? It seems likely that the ability of ANGPTL4 to inhibit LPL is still at work in these tissues. ANGPTL4 has been shown to be important in preventing macrophage foam cell formation [40], in shifting fatty acid delivery from unexercised muscle to exercised muscle [41], and in preventing lipotoxicity in skeletal muscle and heart [42,43]. ANGPTL4 has also been shown to perform roles outside of triglyceride metabolism, and these roles may also be in play [44]. Again, generation of tissue-specific *Angptl4* knockout mice may be necessary to completely address the role of ANGPTL4 in specific tissues.

## CONFLICT OF INTEREST

None declared.

## APPENDIX A. SUPPLEMENTARY DATA

Supplementary data related to this article can be found at http://dx.doi.org/10.1016/j.molmet.2017.06.007

## REFERENCES

[1] Chahil, T.J., Ginsberg, H.N., 2006. Diabetic dyslipidemia. Endocrinology and Metabolism Clinics of North America 35(3):491–510. http://dx.doi.org/10.1016/j.ecl.2006.06.002. vii–viii.

[2] De Man, F.H., Cabezas, M.C., Van Barlingen, H.H., Erkelens, D.W., de Bruin, T.W., 1996. Triglyceride-rich lipoproteins in non-insulin-dependent diabetes mellitus: post-prandial metabolism and relation to premature atherosclerosis. European Journal of Clinical Investigation 26(2):89—108.

[3] Davies, B.S.J., Beigneux, A.P., Barnes II, R.H., Tu, Y., Gin, P., Weinstein, M.M., et al., 2010. GPIHBP1 is responsible for the entry of lipoprotein lipase into capillaries. Cell Metabolism 12(1):42—52. http://dx.doi.org/10.1016/j.cmet.2010.04.016.

[4] Beigneux, A.P., Davies, B.S.J., Gin, P., Weinstein, M.M., Farber, E., Qiao, X., et al., 2007. Glycosylphosphatidylinositol-anchored high density lipoprotein-binding protein 1 plays a critical role in the lipolytic processing of chylomi-crons. Cell Metabolism 5(4):279—291. http://dx.doi.org/10.1016/j.cmet.2007.02.002.

[5] Kersten, S., Mandard, S., Tan, N.S., Escher, P., Metzger, D., Chambon, P., et al., 2000. Characterization of the fasting-induced adipose factor FIAF, a novel peroxisome proliferator-activated receptor target gene. Journal of Biological Chemistry 275(37):28488—28493. http://dx.doi.org/10.1074/jbc.M004029200.

[6] Yoshida, K., Shimizugawa, T., Ono, M., Furukawa, H., 2002. Angiopoietin-like protein 4 is a potent hyperlipidemia-inducing factor in mice and inhibitor of lipoprotein lipase. Journal of Lipid Research 43(11):1770—1772.

[7] Köster, A., Chao, Y.B., Mosior, M., Ford, A., Gonzalez-DeWhitt, P.A., Hale, J.E., et al., 2005. Transgenic angiopoietin-like (angptl)4 overexpression and targeted disruption of angptl4 and angptl3: regulation of triglyceride metabolism. Endocrinology 146(11):4943—4950. http://dx.doi.org/10.1210/en.2005-0476.

[8] Yoon, J.C., Chickering, T.W., Rosen, E.D., Dussault, B., Qin, Y., Soukas, A., et al., 2000. Peroxisome proliferator-activated receptor γ target gene encoding a novel angiopoietin-related protein associated with adipose differentiation. Molecular and Cellular Biology 20(14):5343—5349. http://dx.doi.org/10.1128/MCB.20.14.5343-5349.2000.

[9] Sukonina, V., Lookene, A., Olivecrona, T., Olivecrona, G., 2006. Angiopoietin-like protein 4 converts lipoprotein lipase to inactive monomers and modulates lipase activity in adipose tissue. Proceedings of the National Academy of Sciences of the United States of America 103(46):17450—17455. http://dx.doi.org/10.1073/pnas.0604026103.

[10] Romeo, S., Pennacchio, L.A., Fu, Y., Boerwinkle, E., Tybjaerg-Hansen, A., Hobbs, H.H., et al., 2007. Population-based resequencing of ANGPTL4 uncovers variations that reduce triglycerides and increase HDL. Nature Genetics 39(4):513—516. http://dx.doi.org/10.1038/ng1984.

[11] Dewey, F.E., Gusarova, V., O'Dushlaine, C., Gottesman, O., Trejos, J., Hunt, C., et al., 2016. Inactivating variants in ANGPTL4 and risk of coronary artery disease. New England Journal of Medicine 374(12):1123—1133. http://dx.doi.org/10.1056/NEJMoa1510926.

[12] Genetics, M.I., Investigators, Cardi.E.C., 2016. Coding variation in ANGPTL4, LPL, and SVEP1 and the risk of coronary disease. New England Journal of Medicine 374(12):1134—1144. http://dx.doi.org/10.1056/NEJMoa1507652.

[13] Muendlein, A., Saely, C.H., Leiherer, A., Fraunberger, P., Kinz, E., Rein, P., et al., 2014. Angiopoietin-like protein 4 significantly predicts future cardiovascular events in coronary patients. Atherosclerosis 237(2):632—638. http://dx.doi.org/10.1016/j.atherosclerosis.2014.10.028.

[14] Desai, U., Lee, E.-C., Chung, K., Gao, C., Gay, J., Key, B., et al., 2007. Lipid-lowering effects of anti-angiopoietin-like 4 antibody recapitulate the lipid phenotype found in angiopoietin-like 4 knockout mice. Proceedings of the National Academy of Sciences of the United States of America 104(28):11766—11771. http://dx.doi.org/10.1073/pnas.0705041104.

[15] Lee, E.-C., Desai, U., Gololobov, G., Hong, S., Feng, X., Yu, X.-C., et al., 2009. Identification of a new functional domain in angiopoietin-like 3 (ANGPTL3) and angiopoietin-like 4 (ANGPTL4) involved in binding and inhibition of lipoprotein lipase (LPL). The Journal of Biological Chemistry 284(20):13735—13745. http://dx.doi.org/10.1074/jbc.M807899200.

[16] Kim, J.K., Fillmore, J.J., Chen, Y., Yu, C., Moore, I.K., Pypaert, M., et al., 2001. Tissue-specific overexpression of lipoprotein lipase causes tissue-specific insulin resistance. Proceedings of the National Academy of Sciences of the United States of America 98(13):7522—7527. http://dx.doi.org/10.1073/pnas.121164498.

[17] Wende, A.R., Symons, J.D., Abel, E.D., 2012. Mechanisms of lipotoxicity in the cardiovascular system. Current Hypertension Reports 14(6):517—531. http://dx.doi.org/10.1007/s11906-012-0307-2.

[18] Lichtenstein, L., Mattijssen, F., de Wit, N.J., Georgiadi, A., Hooiveld, G.J., van der Meer, R., et al., 2010. Angptl4 protects against severe proinflammatory effects of saturated fat by inhibiting fatty acid uptake into mesenteric lymph node macrophages. Cell Metabolism 12(6):580—592. http://dx.doi.org/10.1016/j.cmet.2010.11.002.

[19] Tang, T., Li, L., Tang, J., Li, Y., Lin, W.Y., Martin, F., et al., 2010. A mouse knockout library for secreted and transmembrane proteins. Nature Biotechnology 28(7):749—755. http://dx.doi.org/10.1038/nbt.1644.

[20] Young, S.G., Davies, B.S.J., Voss, C.V., Gin, P., Weinstein, M.M., Tontonoz, P., et al., 2011. GPIHBP1, an endothelial cell transporter for lipoprotein lipase. Journal of Lipid Research 52(11):1869—1884. http://dx.doi.org/10.1194/jlr.R018689.

[21] Sanderson, L.M., Degenhardt, T., Koppen, A., Kalkhoven, E., Desvergne, B., Müller, M., et al., 2009. Peroxisome proliferator-activated receptor beta/delta (PPARbeta/delta) but not PPARalpha serves as a plasma free fatty acid sensor in liver. Molecular and Cellular Biology 29(23):6257—6267. http://dx.doi.org/10.1128/MCB.00370-09.

[22] Schmittgen, T.D., Livak, K.J., 2008. Analyzing real-time PCR data by the comparative C(T) method. Nature Protocols 3(6):1101—1108.

[23] Chi, X., Shetty, S.K., Shows, H.W., Hjelmaas, A.J., Malcolm, E.K., Davies, B.S.J., 2015. Angiopoietin-like 4 modifies the interactions between lipoprotein lipase and its endothelial cell transporter GPIHBP1. Journal of Biological Chemistry 290(19):11865—11877. http://dx.doi.org/10.1074/jbc.M114.623769.

[24] Ayala, J.E., Bracy, D.P., McGuinness, O.P., Wasserman, D.H., 2006. Considerations in the design of hyperinsulinemic-euglycemic clamps in the conscious mouse. Diabetes 55(2):390—397.

[25] Davies, B.S.J., Waki, H., Beigneux, A.P., Farber, E., Weinstein, M.M., Wilpitz, D.C., et al., 2008. The expression of GPIHBP1, an endothelial cell binding site for lipoprotein lipase and chylomicrons, is induced by peroxisome proliferator-activated receptor-gamma. Molecular Endocrinology 22(11):2496—2504. http://dx.doi.org/10.1210/me.2008-0146.

[26] Kroupa, O., Vorrsjo, E., Stienstra, R., Mattijssen, F., Nilsson, S.K., Sukonina, V., et al., 2012. Linking nutritional regulation of Angptl4, Gpihbp1, and Lmf1 to lipoprotein lipase activity in rodent adipose tissue. BMC Physiology 12:13. http://dx.doi.org/10.1186/1472-6793-12-13.

[27] Ge, H., Cha, J.-Y., Gopal, H., Harp, C., Yu, X., Repa, J.J., et al., 2005. Differential regulation and properties of angiopoietin-like proteins 3 and 4. Journal of Lipid Research 46(7):1484—1490. http://dx.doi.org/10.1194/jlr.M500005-JLR200.

[28] Badman, M.K., Pissios, P., Kennedy, A.R., Koukos, G., Flier, J.S., Maratos-Flier, E., 2007. Hepatic fibroblast growth factor 21 is regulated by PPARalpha and is a key mediator of hepatic lipid metabolism in ketotic states. Cell Metabolism 5(6):426—437. http://dx.doi.org/10.1016/j.cmet.2007.05.002.

[29] Inagaki, T., Dutchak, P., Zhao, G., Ding, X., Gautron, L., Parameswara, V., et al., 2007. Endocrine regulation of the fasting response by PPARalpha-mediated induction of fibroblast growth factor 21. Cell Metabolism 5(6):415—425. http://dx.doi.org/10.1016/j.cmet.2007.05.003.

[30] Palou, M., Priego, T., Sánchez, J., Villegas, E., Rodríguez, A.M., Palou, A., et al., 2008. Sequential changes in the expression of genes involved in lipid metabolism in adipose tissue and liver in response to fasting. Pflügers Archiv — European Journal of Physiology 456(5):825. http://dx.doi.org/10.1007/s00424-008-0461-1.

[31] Hultin, M., Carneheim, C., Rosenqvist, K., Olivecrona, T., 1995. Intravenous lipid emulsions: removal mechanisms as compared to chylomicrons. Journal of Lipid Research 36(10):2174–2184.

[32] Laplante, M., Festuccia, W.T., Soucy, G., Blanchard, P.-G., Renaud, A., Berger, J.P., et al., 2009. Tissue-specific postprandial clearance is the major determinant of PPARγ-induced triglyceride lowering in the rat. American Journal of Physiology — Regulatory, Integrative and Comparative Physiology 296(1):R57–R66. http://dx.doi.org/10.1152/ajpregu.90552.2008.

[33] Kusminski, C.M., Holland, W.L., Sun, K., Park, J., Spurgin, S.B., Lin, Y., et al., 2012. MitoNEET-driven alterations in adipocyte mitochondrial activity reveal a crucial adaptive process that preserves insulin sensitivity in obesity. Nature Medicine 18(10):1539–1549. http://dx.doi.org/10.1038/nm.2899.

[34] Rensen, P.C., van Dijk, M.C., Havenaar, E.C., Bijsterbosch, M.K., Kruijt, J.K., van Berkel, T.J., 1995. Selective liver targeting of antivirals by recombinant chylomicrons — a new therapeutic approach to hepatitis B. Nature Medicine 1(3):221–225.

[35] Bruns, O.T., Ittrich, H., Peldschus, K., Kaul, M.G., Tromsdorf, U.I., Lauterwasser, J., et al., 2009. Real-time magnetic resonance imaging and quantification of lipoprotein metabolism in vivo using nanocrystals. Nature Nanotechnology 4(3):193–201. http://dx.doi.org/10.1038/nnano.2008.405.

[36] Sonnenburg, W.K., Yu, D., Lee, E.-C., Xiong, W., Gololobov, G., Key, B., et al., 2009. GPIHBP1 stabilizes lipoprotein lipase and prevents its inhibition by angiopoietin-like 3 and angiopoietin-like 4. Journal of Lipid Research 50(12): 2421–2429. http://dx.doi.org/10.1194/jlr.M900145-JLR200.

[37] Dijk, W., Beigneux, A.P., Larsson, M., Bensadoun, A., Young, S.G., Kersten, S., 2016. Angiopoietin-like 4 promotes intracellular degradation of lipoprotein lipase in adipocytes. Journal of Lipid Research 57(9):1670–1683. http://dx.doi.org/10.1194/jlr.M067363.

[38] Kersten, S., 2014. Physiological regulation of lipoprotein lipase. Biochimica Et Biophysica Acta 1841(7):919–933. http://dx.doi.org/10.1016/j.bbalip.2014.03.013.

[39] Zhang, R., Abou-Samra, A.B., 2014. A dual role of lipasin (betatrophin) in lipid metabolism and glucose homeostasis: consensus and controversy. Cardiovascular Diabetology 13:133. http://dx.doi.org/10.1186/s12933-014-0133-8.

[40] Aryal, B., Rotllan, N., Araldi, E., Ramírez, C.M., He, S., Chousterman, B.G., et al., 2016. ANGPTL4 deficiency in haematopoietic cells promotes monocyte expansion and atherosclerosis progression. Nature Communications 7:12313. http://dx.doi.org/10.1038/ncomms12313.

[41] Catoire, M., Alex, S., Paraskevopulos, N., Mattijssen, F., Evers-Van Gogh, I., Schaart, G., et al., 2014. Fatty acid-inducible ANGPTL4 governs lipid metabolic response to exercise. Proceedings of the National Academy of Sciences of the United States of America 111(11):E1043–E1052. http://dx.doi.org/10.1073/pnas.1400889111.

[42] Klingler, C., Zhao, X., Adhikary, T., Li, J., Xu, G., Häring, H.-U., et al., 2016. Lysophosphatidylcholines activate PPARδ and protect human skeletal muscle cells from lipotoxicity. Biochimica Et Biophysica Acta 1861(12 Pt A):1980–1992. http://dx.doi.org/10.1016/j.bbalip.2016.09.020.

[43] Puthanveetil, P., Wan, A., Rodrigues, B., 2015. Lipoprotein lipase and angiopoietin-like 4-cardiomyocyte secretory proteins that regulate metabolism during diabetic heart disease. Critical Reviews in Clinical Laboratory Sciences 52(3):138–149. http://dx.doi.org/10.3109/10408363.2014.997931.

[44] Gray, N.E., Lam, L.N., Yang, K., Zhou, A.Y., Koliwad, S., Wang, J.-C., 2012. Angiopoietin-like 4 (Angptl4) protein is a physiological mediator of intracellular lipolysis in murine adipocytes. The Journal of Biological Chemistry 287(11): 8444–8456. http://dx.doi.org/10.1074/jbc.M111.294124.